Rotationally Inelastic Collisions of CN(A 2 Π) with Small Molecules †

ARTICLE *in* THE JOURNAL OF PHYSICAL CHEMISTRY A · MAY 2009

Impact Factor: 2.69 · DOI: 10.1021/jp901925s · Source: PubMed

Rotationally Inelastic Collisions of CN($A^2\Pi$) with Small Molecules†

Ani Khachatrian and Paul J. Dagdigian*

Department of Chemistry, The Johns Hopkins University, Baltimore, Maryland 21218-2685

Received: March 2, 2009; Revised Manuscript Received: April 3, 2009

An optical−optical double resonance technique has been utilized to investigate rotational energy transfer of selected rotational/fine-structure levels of CN($A^2\Pi$, $v = 3$) in collisions with the molecular partners CO_2 and CH_4. Total removal rate constants for several rotational/fine-structure levels were measured for both collision partners. State-to-state relative rate constants were determined for several initial levels. These show a strikingly strong collisional propensity to conserve the fine-structure/Λ-doublet label, akin to our previous observations with the N_2 collision partner. The possible origin of this propensity is discussed.

1. Introduction

Rotational energy transfer is a facile collision process that plays a key role in many environments and has been extensively studied both theoretically and experimentally. Of special interest are collisions of molecules in open-shell electronic states, because of the differing effect of collisions upon the rotational angular momentum and the fine-structure/Λ-doublet labels.[1] Modern experimental techniques utilizing molecular beams and/or lasers have been employed to study rotationally inelastic collisions between specified initial and final rotational/fine-structure levels in open-shell electronic states.[2,3] There have been parallel advances in the theoretical treatment of the inelastic collision dynamics[4] and in the computation of state-to-state cross sections.

Several investigations of state-resolved rotational energy transfer in the ground and first two excited states of the CN radical have been carried out. Sadowski, Smith, and their co-workers have determined state-to-state rate constants for collisions of CN in the $X\,^2\Sigma^+$ and $B^2\Sigma^+$ electronic states. Collisions of these Σ molecular electronic states require only a single potential energy surface (PES) to describe the interaction with a collision partner. Fei et al.[5,6] have employed stimulated emission pumping to prepare specific initial rotational levels in the CN($X\,^2\Sigma^+$, $v = 2$) vibrational manifold in studies of rotational energy transfer in collisions with He and Ar. Smith and co-workers[7–9] have employed IR−visible double resonance to determine total removal and state-to-state rate constants for collisions of selected CN($X\,^2\Sigma^+$, $v = 2$) rotational levels with N_2 and C_2H_2. Sadowski and co-workers[10,11] utilized selective laser excitation and resolved fluorescence spectroscopy to study rotational energy transfer within the CN($B^2\Sigma^+$) electronic state. In these studies of rotational energy transfer within CN $^2\Sigma^+$ electronic states, the spin splittings of the rotational levels were not resolved.

Our laboratory and McKendrick and co-workers have investigated state-resolved collisions of CN($A^2\Pi$). McKendrick and co-workers[12] have recently implemented Doppler-resolved frequency-modulated spectroscopy to investigate state-resolved collisions of CN($A^2\Pi$) with velocity resolution. This technique has been employed to determine state-to-state differential cross sections.[13]

In collaboration with theoretical work by Alexander and his co-workers, we have carried out an extensive series of state-to-state studies of rotational and electronic transfer of CN in its first, $A^2\Pi$, electronic state in collisions mainly with rare gases.[14–23] The experimental studies employed the optical−optical double resonance technique to prepare specific CN($A^2\Pi$) rotational/fine-structure levels and to detect the populations of the collisionally populated levels. In contrast to collisions of a molecule in a Σ state, collisions of molecules in Π states necessarily involve two Born−Oppenheimer potential energy surfaces (PES's), since the orbital degeneracy of the Π state is removed by the approach of the collision partner.[4] The two PES's correspond to atom−diatom electronic wave functions of A' and A'' symmetry. The determination of accurate ab initio PES's for the interaction of CN($A^2\Pi$) with spherical collision partners is now possible, especially if one neglects the dependence of the PES's on the CN bond length. Quantum scattering calculations with computed PES's have allowed comparison of predicted state-to-state rate constants with experimental measurements. In collisions of low rotational levels of CN($A^2\Pi$, v=3) with Ar, a significant propensity to change the fine-structure and Λ-doublet labels was experimentally observed and similarly found in the calculations.[21]

In a recent study, we extended our collaborative effort with Alexander's group to the study of state-resolved CN($A^2\Pi$) rotational energy transfer to a molecular partner, namely N_2.[23] The experimentally determined state-to-state rate constants display a strikingly strong propensity to conserve the fine-structure/Λ-doublet label, in contrast to CN($A^2\Pi$)-Ar collisions. These experimental data were compared with the results of quantum scattering calculations based on PES's averaged over the orientation of the N_2 molecule. A much stronger probability for fine-structure and Λ-doublet changing transitions was found in the computed state-to-state rate constants than was observed experimentally. It is possible that this difference between experiment and theory results from neglect, in the theoretical treatment, of the N_2 orientation and, in particular, the correlation of CN and N_2 angular motion.

In view of the experimentally observed[23] strong conservation of the CN fine-structure/Λ-doublet label in CN($A^2\Pi$)−N_2 collisions, it is of interest to investigate whether there is a similar propensity in rotationally inelastic collisions of CN($A^2\Pi$) with other small molecules. In the present work, we report a state-

† Part of the "Robert W. Field Festschrift".

* To whom correspondence should be addressed. Fax: (410) 516-8420. E-mail: pjdagdigian@jhu.edu.

10.1021/jp901925s CCC: $40.75
Published on Web 04/30/2009

to-state study of rotational energy transfer in CN($A^2\Pi$) in collisions with the molecular targets CO_2 and CH_4.

2. Experimental Section

The apparatus with which this study was conducted has been described in detail previously,[23] and only a brief description is presented here. Optical−optical double resonance (OODR) was employed for the study of rotationally inelastic collisions of CN($A^2\Pi$, $v = 3$) with resolution of the initial and final rotational/fine-structure levels. CN radicals were generated in a slow flow of the molecular collision partner (CO_2 or CH_4) in a reaction cell by 193 nm excimer laser photolysis of BrCN (Sigma Aldrich, 99.995%). Typical partial pressures were 0.004 Torr of BrCN and 0.3 Torr for the collision partner.

The tunable pulsed pump and probe lasers (pulse widths ~8 ns) were overlapped with a dichroic mirror and counterpropagated with the excimer laser beam through the reaction chamber. The pump laser was tuned to an isolated rotational line in the CN $A^2\Pi-X\,^2\Sigma^+$ (3,0) band at 694 nm to excite molecules to a given rotational/fine-structure level in the $v_A = 3$ vibronic manifold. The probe laser, which was delayed after the pump laser, was scanned in wavelength through the $B^2\Sigma^+-A^2\Pi$ (3,3) band at 567 nm to detect the initially excited and collisionally populated levels within $v_A = 3$.

The pump and probe laser pulses were delayed by 200 μs after the excimer laser so that the CN($X\,^2\Sigma^+$) radicals had relaxed to room temperature translational and rotational state distributions.[8,23] Olkhov and Smith[8] considered in detail the thermalization of CN in rotational energy transfer studies of CN($X\,^2\Sigma^+$, $v = 2$) in collisions with N_2 in a cell. They employed two different sources of CN, namely 266 nm photolysis of ICN, which produces translationally hot radicals, and 570 nm photolysis of NCNO, which yields radicals with a near room temperature translational energy distribution. They found that the CN(X)−N_2 total removal rate constants with NCNO precursor were essentially independent of the photolysis-probe delay, while rate constants with the ICN precursor were larger for short delays and approach values with NCNO precursor for pressure−time products of ~1 Torr·μs. Similar to ICN, photolysis of BrCN produces translationally hot radicals. With a pressure of 0.3 Torr of CO_2 and a long delay (200 μs), the CN radicals in our experiment are well equilibrated translationally. Hence, the average relative collision energy for both targets was (3/2)kT, or 313 cm^{-1}.

Two separate photomultiplier detectors observed the laser-induced fluorescence: one monitored the $A-X$ fluorescence excited by the pump laser, while the second observed the $B-X$ OODR signal excited by the probe laser. The transient signals from the photomultipliers were directed to gated integrators, whose outputs were collected under computer control.

The pulse energy of the pump laser (7 mJ in a 1.5 mm diameter beam entering the chamber) was sufficiently high to saturate the $A-X$ transition, so that the initially excited rotational level had an isotropic M_J state distribution. The probe laser pulse energy (0.5 mJ in a 1.5 mm diameter beam) was sufficiently high that line strength factors appropriate to saturation conditions[24] for the main-branch ($F_i \leftarrow F_i$) lines[25] [P_i, Q_i, R_i, $i = 1$ and 2] could be used to convert line intensities in the OODR spectra to populations. In addition to the main branches, there are several branches in which the fine-structure label is different for the upper and lower level. These include the R_{21} branch ($\Delta J = +1$, $F_2 \leftarrow F_1$), which was used to observe one of the initial levels studied (see below).

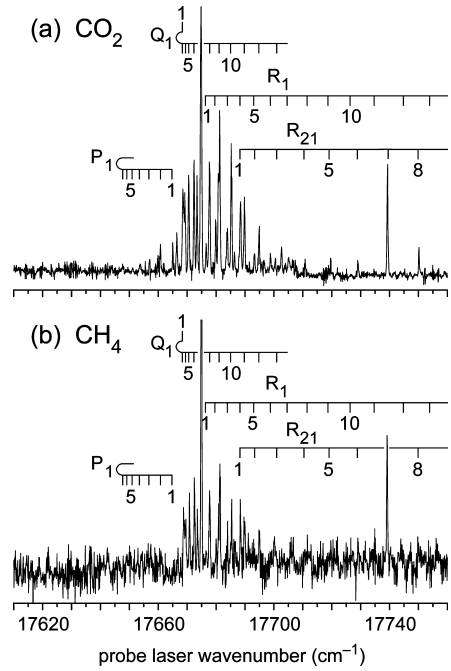

Figure 1. OODR $B^2\Sigma^+-X\,^2\Sigma^+$ laser-induced fluorescence spectra of the CN $B^2\Sigma^+-A^2\Pi$ (3,3) band, with (a) CO_2 and (b) CH_4 collision partners. For both spectra, the $J = 7.5$ F_1f initial level was prepared by pump laser excitation of the $Q_1(7)$ line of the $A^2\Pi-X\,^2\Sigma^+$ (3,0) band, with pump−probe delays of 10 ns. The partial pressure of the BrCN photolytic precursor and the collision partner was 0.004 and 0.3 Torr, respectively, and the photolysis-pump delay was 200 μs. The rotational lines are identified with the rotational angular momentum N of the CN($A^2\Pi$, $v = 3$) levels.

3. Results

We investigated state-to-state collisions of lower rotational/fine-structure levels of the CN($A^2\Pi$, $v = 3$) manifold. These rotational levels are fairly close to the Hund's case (a) limit.[26] In this case, the electron spin is strongly coupled to the internuclear axis and hence to the electronic orbital angular momentum projection Λ. This gives rise to two fine-structure manifolds, with molecular-fixed projection $\Omega = \Lambda + \Sigma = {}^1/_2$ and ${}^3/_2$. Because the spin−orbit constant A is negative[26] for CN($A^2\Pi$), the lower (in energy) of these two manifolds, labeled F_1, corresponds to $\Omega = {}^3/_2$ and the upper, labeled F_2, to $\Omega = {}^1/_2$. Because of the orbital degeneracy of the $A^2\Pi$ state, the rotational levels appear as nearly degenerate pairs (Λ-doublets) of opposite total parity, which are labeled[27] e and f for total parity $+(-1)^{J-1/2}$ and $-(-1)^{J-1/2}$, respectively.

Panels a and b of Figure 1 presents OODR spectra recorded at a short, 10 ns pump−probe delay for the $J = 7.5$ F_1f initial level with CO_2 and CH_4 as the collision partner, respectively. A pump−probe delay that is short compared to an estimated 200 ns average time between collisions was employed. In this way, the densities of the collisionally populated levels were not affected significantly by secondary collisions, and the populations of these levels are proportional to the state-to-state rate constants (see, for example, ref 28).

The signal-to-noise ratio for the OODR spectrum in Figure 1b is poorer than that presented in Figure 1a. This presumably results from a somewhat lower concentration of CN($X\,^2\Sigma^+$) radicals in the apparatus because CH_4, in contrast to CO_2, reacts appreciably with the radical. Taking the literature value[29] for the CN−CH_4 room temperature reaction rate constant, the concentration of photolytically generated CN is computed to decrease by a factor of 3.6 during the 200 μs photolysis-pump delay at a CH_4 partial pressure of 0.3 Torr.

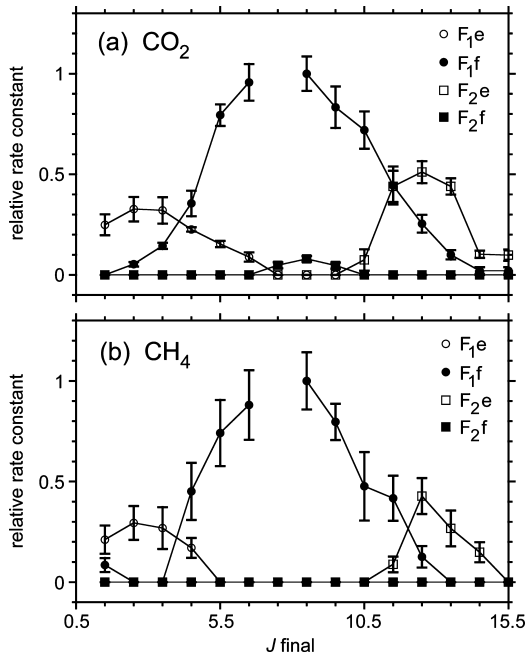

Figure 2. Relative room temperature rate constants for transfer out of the $J = 7.5$ F_1f level of CN($A^2\Pi$, $v = 3$) in collisions with (a) CO_2 and (b) CH_4. The rate constants for each collision partner have been normalized to that of the $J = 7.5$ $F_1f \rightarrow J = 8.5$ F_1f transition. The fine-structure/Λ-doublet label of each final level is indicated with the symbols noted in the figure.

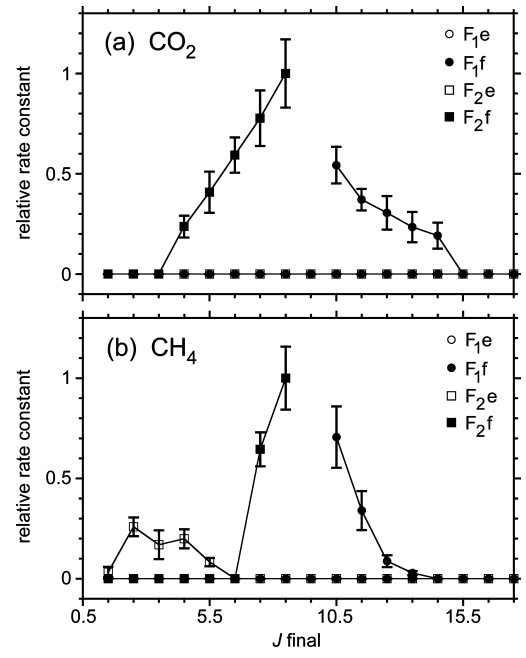

Figure 3. Relative room temperature rate constants for transfer out of the $J = 9.5$ F_2f level of CN($A^2\Pi$, $v = 3$) in collisions with (a) CO_2 and (b) CH_4. The rate constants for each collision partner have been normalized to that of the $J = 9.5$ $F_2f \rightarrow J = 8.5$ F_2f transition. The fine-structure/Λ-doublet label of each final level is indicated with the symbols noted in the figure.

The most intense line in both OODR spectra displayed in Figure 1 is the $Q_1(7)$ line. Also prominent in the spectra is the $R_{21}(7)$ line. The lower level of both of these lines is the initial $J = 7.5$ F_1f level, prepared by pump laser excitation. The most intense so-called "satellite" lines, i.e., those involving detection of collisionally populated rotational/fine-structure levels within $v_A = 3$, are in the Q_1 branch, which probe levels with the same fine-structure/Λ-doublet level as the initial level. Some lines in the P_1 and R_1 branch, for low J, also appear weakly in the OODR spectra. With the exception of several lines in the Q_2 branch near the $Q_1(7)$ line, lines probing levels in the F_2 fine-structure manifold were very weak or not observed. (The P_2 band head occurs at a transition wavenumber of 17611 cm^{-1} and degrades to higher wavenumber.) OODR spectra were taken for other initial levels, and these show a similar absence of appreciable intensity in lines probing fine-structure/Λ-doublet levels other than that of the initial level.

Spectra such as those shown in Figure 1 were used to determine relative state-to-state rate constants for collision-induced rotational transitions from several initial levels with both collision partners. Figure 2 presents derived rate constants for collisional transfer out of the $J = 7.5$ F_1f level with CO_2 and CH_4 as collision partners. These data were derived from rotational line intensities in OODR spectra such as those shown in Figure 1. The largest rate constants are for transitions to other F_1f rotational levels, which conserve both the fine-structure and Λ-doublet labels. Low-J lines in the P_1 and R_1 branches are also weaker with significantly weaker intensities. With the exception of several lines in the Q_2 branch near the $Q_1(7)$ line, lines probing levels in the F_2 fine-structure manifold were very weak or not observed at short pump−probe delays. Thus, the line intensities in the OODR spectra strongly suggest a substantial propensity to conserve the fine-structure/Λ-doublet label, as we have also observed in CN(A)−N_2 collisions.[23]

Figure 3 presents derived state-to-state rate constants for collisional transfer out of the $J = 9.5$ F_2f initial level. These data display the very strong propensity for conversation of the fine-structure/Λ-doublet label which was qualitatively inferred from the relative intensities in the OODR spectra. Comparing the rate constants in Figures 2 and 3, we note in particular that this propensity is much stronger for the $J = 9.5$ F_2f level than for the $J = 7.5$ F_1f level.

4. Discussion

In addition to rotational energy transfer, other processes, including electronic quenching and chemical reaction, are possible in collisions of CN($A^2\Pi$) with CO_2 and CH_4. Previous studies have reported room temperature rate constants for chemical reaction and electronic quenching of CN with CO_2 and CH_4. The CN($X\,^2\Sigma^+$) + $CO_2 \rightarrow$ NCO + CO reaction was investigated over a wide temperature range by Balla and Castleton.[30] The reaction rate was not measurable for $T < 900$ K, and they report an upper limit of 2×10^{-15} cm^3 $molecule^{-1}$ s^{-1} for the room temperature rate constant, in agreement with earlier work by Jacobs et al.[31] but in disagreement with a rate constant of $(2.3 \pm 0.4) \times 10^{-14}$ cm^3 $molecule^{-1}$ s^{-1} reported by Li et al.[32] Taherian and Slanger[33] determined a rate constant of $(2.5 \pm 0.15) \times 10^{-11}$ cm^3 $molecule^{-1}$ s^{-1} for the electronic quenching of CN($A^2\Pi$, $v = 1$) by CO_2. The ground state CN($X\,^2\Sigma^+$) radical has been found to react with CH_4, with a room temperature rate constant of 8.5×10^{-13} cm^3 $molecule^{-1}$ s^{-1}, yielding HCN + CH_3 products.[29] To our knowledge, electronic quenching of CN($A^2\Pi$) by CH_4 has not been investigated. Our observation of OODR spectra with both CO_2 and CH_4 collision partners indicates that the removal of CN($A^2\Pi$) radicals by electronic quenching or chemical reaction does not dominate the loss of the electronically excited radical as compared to other loss mechanisms such as radiative decay and physical diffusion.

The present results and our previous investigation of CN(A)−N_2 collisions[23] reveal a strong propensity to conserve

the fine-structure/Λ-doublet label in rotationally inelastic collisions of CN($A^2\Pi$, $v = 3$) with the molecular targets N_2, CO_2, and CH_4. This propensity differs markedly with our previous experiments and quantum scattering calculations on collisions of CN($A^2\Pi$, $v = 3$) with the inert atomic gas Ar.[21] For this spherical collision partner, significant state-to-state rate constants for transitions into all four of the fine-structure/Λ-doublet manifolds were found.

Alexander and co-workers[4,34] have derived propensity rules for changes of the fine-structure and Λ-doublet labels in collisions of a molecule in a $^2\Pi$ electronic state from a general consideration of the quantum scattering equations. In the Hund's case (a) limit, which applies to the rotational/fine-structure levels investigated here, rotationally inelastic transitions which conserve the fine-structure/Λ-doublet label are enabled by the anisotropic part of the sum (V_{sum}) of the A' and A'' PES's, while the difference (V_{diff}) of the PES's is responsible for fine-structure changing transitions.

Our observation of strong conservation of the fine-structure and Λ-doublet labels could be taken to imply that V_{diff} is relatively small compared to V_{sum} for the interaction of CN($A^2\Pi$) with these molecular collision partners. In the case of N_2, this supposition was tested through ab initio calculation of CN($A^2\Pi$)−N_2 PES's by Alexander and co-workers.[23] Calculation of PES's for this diatom−diatom system is much more demanding than that for an atom−diatom system. First, the PES's depend on more nuclear coordinates. More importantly, there are no symmetry elements for a general diatom−diatom geometry, so that both PES's involve states of A_1 symmetry, except for special geometries. To make progress on this molecule−molecule system, Alexander and co-workers computed PES's for three orientations of the N_2 molecule for which the system has a plane of symmetry. They further replaced the diatom−diatom PES's by the interaction of CN with a spherically averaged N_2 molecule, carried out through averaging over the PES's computed for the three N_2 orientations. For the averaged PES's, the value of V_{diff} ranges from 0 to ∼350 cm^{-1} as a function of the Jacobi angle for a separation R for which V_{sum} equals 300 cm^{-1} (approximately the average room temperature collision energy). [It should be noted that V_{diff} is zero at linear geometries.]

In our collaborative study of CN($A^2\Pi$)−N_2 collisions,[23] the experimentally determined relative state-to-state rate constants were compared with rate constants computed with the averaged PES's described above. The computed rate constants were found to be large for both Λ-doublet conserving and changing transitions which conserved fine-structure label. Somewhat smaller, but significant, rate constants were computed for fine-structure changing transitions. Thus, the calculations do not predict the strong propensity to conserve the fine-structure and Λ-doublet label, seen in the experimentally determined state-to-state rate constants.

It is of interest to compare our observations on CN($A^2\Pi$)−molecule collisions with those of ter Meulen and co-workers on OH($X^2\Pi$)−molecule collisions.[35,36] In their experiment, hexapole state selection was employed to prepare OH in a single Λ-doublet level ($J = 1.5$ $F_1 f$). This state-selected beam was collided with a beam of the collision partner, and the collisionally populated rotational/fine-structure levels were probed by laser-induced fluorescence. Ter Meulen and co-workers have applied this technique to rotationally inelastic collisions of OH with a variety of molecular collision partners, including CO_2. In all cases, they observe a significant probability to populate the upper (F_2) fine-structure manifold. Unequal Λ-doublet populations were also found in fine-structure conserving transitions, but Λ-doublet conservation was not observed. The collisional propensities for OH($X^2\Pi$) and CN($A^2\Pi$) thus appear to be quite different.

It is possible, in principle, that the observed propensity to conserve the fine-structure/Λ-doublet label in CN($A^2\Pi$)−molecule collisions is due to the long-range part of the PES's. The CN($A^2\Pi$) dipole moment is quite small in comparison with that of the ground $X\,^2\Sigma^+$ state [$\mu = 0.3$ vs. 1.3 D].[37] To our knowledge, the quadrupole moment for CN($A^2\Pi$) has not been reported; the value for CN($X\,^2\Sigma^+$) has been computed to equal $\Theta = 0.59$ D·Å.[38] Since the CN($A^2\Pi$) dipole moment is small, the leading long-range interaction with the molecular collision partners is the quadrupole−quadrupole interaction. The quadrupole moment of CO_2 is significantly larger in magnitude than that of N_2 [$\Theta = -4.28$ vs. -1.40 D·Å].[39] The quadrupole−quadrupole interaction can enable both fine-structure conserving and changing transitions.[40] Within a given fine-structure manifold, this interaction (with $l = 4$ anisotropy) directly couples[4,41] Λ-doublets of the same *e/f* symmetry for ΔJ even and opposite parity for ΔJ odd and hence does not provide an explanation for the observed strong propensity for conservation of the fine-structure Λ-doublet label in CN($A^2\Pi$)−molecule collisions. Because of symmetry, CH_4 has no quadrupole moment, and the leading long-range interaction of CH_4 with CN($A^2\Pi$) is the dispersion interaction. Differential cross section measurements, such as those carried out by McKendrick and co-workers,[13] could be useful in determining the importance of long-range interactions in the rotationally inelastic collisions.

A more refined theoretical treatment of the collision dynamics is needed to understand the observed propensity to conserve the fine-structure/Λ-doublet label. Perhaps the distinctive feature of these molecule−molecule systems which leads to a strong propensity to conserve the CN fine-structure/Λ-doublet label is the correlation of the angular motions of the two molecules. We encourage exploratory ab initio investigation of the PES's for the CN−CO_2 and CN−CH_4 systems.

Acknowledgment. The authors appreciate the encouragement and comments of Millard Alexander.

References and Notes

(1) Alexander, M. H. *J. Chem. Phys.* **1982**, *76*, 5974.
(2) Liu, K.; Macdonald, R. G.; Wagner, A. F. *Int. Rev. Phys. Chem.* **1990**, *9*, 187.
(3) Dagdigian, P. J. In *The Chemical Dynamics and Kinetics of Small Radicals, Part I*; Liu, K., Wagner, A. F., Eds.; World Scientific: Singapore, 1995; p 315.
(4) Alexander, M. H. *Chem. Phys.* **1985**, *92*, 337.
(5) Fei, R.; Lambert, H. M.; Carrington, T.; Filseth, S. V.; Sadowski, C. M. *J. Chem. Phys.* **1994**, *100*, 1190.
(6) Fei, R.; Adelman, D. E.; Carrington, T.; Dugan, C. H.; Filseth, S. V. *Chem. Phys. Lett.* **1995**, *232*, 547.
(7) Hickson, K. M.; Sadowski, C. M.; Smith, I. W. M. *Chem. Phys. Lett.* **2003**, *372*, 443.
(8) Olkhov, R. V.; Smith, I. W. M. *Phys. Chem. Chem. Phys.* **2006**, *8*, 5643.
(9) Olkhov, R.; Smith, I. W. M. *J. Chem. Phys.* **2007**, *126*, 134314.
(10) Guo, J. Z.; Sadowski, C. M.; Gao, Q.; Morgan, F. J. *J. Chem. Phys.* **2000**, *113*, 7276.
(11) Brunet, S. M. K.; Guo, J. Z.; Carrington, T.; Filseth, S. V.; Sadowski, C. M. *J. Chem. Phys.* **2002**, *116*, 3617.
(12) Alagappan, A.; Ballingall, I.; Costen, M. L.; McKendrick, K. G.; Paterson, G. *Phys. Chem. Chem. Phys.* **2007**, *9*, 747.
(13) Alagappan, A.; Ballingall, I.; Costen, M. L.; McKendrick, K. G. *J. Chem. Phys.* **2007**, *126*, 041103.
(14) Furio, N.; Ali, A.; Dagdigian, P. J. *Chem. Phys. Lett.* **1986**, *125*, 561.
(15) Furio, N.; Ali, A.; Dagdigian, P. J. *J. Chem. Phys.* **1986**, *85*, 3860.

(16) Jihua, G.; Ali, A.; Dagdigian, P. J. *J. Chem. Phys.* **1986**, *85*, 7098.
(17) Ali, A.; Jihua, G.; Dagdigian, P. J. *J. Chem. Phys.* **1987**, *87*, 2045.
(18) Dagdigian, P. J.; Patel-Misra, D.; Berning, A.; Werner, H.-J.; Alexander, M. H. *J. Chem. Phys.* **1993**, *98*, 8580.
(19) Yang, X.; Dagdigian, P. J. *Chem. Phys. Lett.* **1998**, *297*, 506.
(20) Yang, X.; Dagdigian, P. J.; Alexander, M. H. *J. Chem. Phys.* **2000**, *112*, 4474.
(21) Alexander, M. H.; Yang, X.; Dagdigian, P. J.; Berning, A.; Werner, H.-J. *J. Chem. Phys.* **2000**, *112*, 781.
(22) Nizamov, B.; Dagdigian, P. J.; Alexander, M. H. *J. Chem. Phys.* **2001**, *115*, 8393.
(23) Khachatrian, A.; Dagdigian, P. J.; Bennett, D. I. G.; Lique, F.; Klos, J.; Alexander, M. H. *J. Phys. Chem. A* **2009**, *113*, 3922.
(24) Guyer, D. R.; Hüwel, L.; Leone, S. R. *J. Chem. Phys.* **1983**, *83*, 1259.
(25) Herzberg, G. *Molecular Spectra and Molecular Structure I. Spectra of Diatomic Molecules*, 2nd ed.; D. Van Nostrand: Princeton, NJ, 1950.
(26) Kotlar, A. J.; Field, R. W.; Steinfeld, J. I.; Coxon, J. A. *J. Mol. Spectrosc.* **1980**, *80*, 86.
(27) Brown, J. M.; Hougen, J. T.; Huber, K.-P.; Johns, J. W. C.; Kopp, I.; Lefebvre-Brion, H.; Merer, A. J.; Ramsay, D. A.; Rostas, J.; Zare, R. N. *J. Mol. Spectrosc.* **1975**, *55*, 500.
(28) Kind, M.; Stuhl, F. *J. Chem. Phys.* **2001**, *114*, 6160.
(29) Baulch, D. L.; Conos, C. J.; Cox, R. A.; Frank, P.; Hayman, G.; Just, Th.; Kerr, J. A.; Murrells, T.; Pilling, M. J.; Troe, J.; Walker, R. W.; Warnatz, J. *J. Phys. Chem. Ref. Data* **1994**, *23*, 847.
(30) Balla, R. J.; Castleton, K. H. *J. Phys. Chem.* **1991**, *95*, 2344.
(31) Jacobs, A.; Wahl, M.; Weller, R.; Wolfrum, J. In *Twenty-second Symposium (International) on Combustion*; Combustion Institute: Pittsburgh, PA, 1988; p 1093.
(32) Li, X.; Sayah, N.; Jackson, W. M. *J. Chem. Phys.* **1984**, *81*, 833.
(33) Taherian, M. R.; Slanger, T. G. *J. Chem. Phys.* **1985**, *82*, 2511.
(34) Corey, G. C.; Alexander, M. H. *J. Chem. Phys.* **1986**, *85*, 5652.
(35) van Beek, M. C.; Schreel, K.; ter Meulen, J. J. *J. Chem. Phys.* **1998**, *109*, 1302.
(36) Moise, A.; Parker, D. H.; ter Meulen, J. J. *J. Chem. Phys.* **2007**, *126*, 124302.
(37) Knowles, P. J.; Werner, H.-J.; Hay, P. J.; Cartwright, D. C. *J. Chem. Phys.* **1988**, *89*, 7334.
(38) Bruna, P. J.; Grein, F. *J. Chem. Phys.* **2007**, *127*, 074107.
(39) Graham, C.; Imrie, D. A.; Raab, R. E. *Mol. Phys.* **1998**, *93*, 49.
(40) Miller, S. M.; Clary, D. C. *J. Chem. Phys.* **1993**, *98*, 1843.
(41) Dagdigian, P. J.; Alexander, M. H.; Liu, K. *J. Chem. Phys.* **1989**, *91*, 839.

JP901925S